

7

Dynamics of domain walls

In this chapter we discuss the dynamics of kinks and domain walls first in the zero thickness approximation, and then briefly in the full field theory. The zero thickness approximation can be expected to be valid in the case when all other length scales, such as the radii of curvature of a domain wall, are much larger than the wall thickness.¹ We start by deriving the action for a kink in 1 + 1 dimensions as this is the simplest case and contains the essential features of the higher dimensional cases. Then we derive the action for a domain wall in 3 + 1 dimensions and some consequences. In this chapter we ignore gravitational effects which can be quite important in certain situations (see Chapter 8).

7.1 Kinks in 1 + 1 dimensions

In 1 + 1 dimensions, if we ignore the structure of the kink, then we expect the kink to behave simply as a massive point particle. Its dynamics are then given by the usual action for a massive point particle

$$S_{1+1} = -M \int d\tau \quad (7.1)$$

where M is the mass of the kink and $d\tau$ is the line element which may also be written as

$$d\tau = dt \left(g_{\mu\nu} \frac{dX^\mu}{dt} \frac{dX^\nu}{dt} \right)^{1/2} \quad (7.2)$$

where $g_{\mu\nu}$ is the metric of the space-time background and $X^\mu(t)$ is the location of the kink at time t .

While the action in Eq. (7.1) seems reasonable on physical grounds, there should be a systematic way to derive it starting from the original field theory action of which

¹ This expectation is not completely correct since the wall velocity is also important [183, 73].

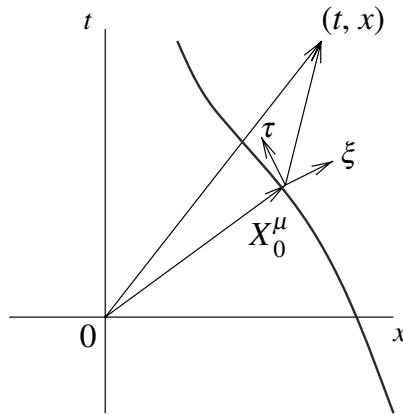


Figure 7.1 The world-line of the kink is represented by the curve. The kink frame coordinates $y^a = (\tau, \xi)$ are defined in the instantaneous rest frame of the kink and are functions of the background coordinates $x^\mu = (t, x)$.

the kink is a solution. Such a derivation should lead to Eq. (7.1) plus corrections that depend on the internal structure of the kink.

To derive the effective action (Eq. (7.1)), the key assumption is that the field profile of the kink is well-approximated by that of the known static kink solution in the instantaneous rest frame of the kink. To proceed with the derivation, we work in “kink frame coordinates” which are denoted by $y^a = (\tau, \xi)$, $a = 0, 1$, as illustrated in Fig. 7.1 (τ is also called the kink world-line coordinate). These coordinates are functions of the background coordinates that are denoted by $x^\mu = (t, x)$, $\mu = 0, 1$.

The kink world-line is given by the position 2-vector $X^\mu = (t, X(t))$. Therefore the vector tangent to the world-line is $T^\mu = N_T(1, \partial_t X)$ where N_T is a normalization factor chosen to enforce

$$g_{\mu\nu} T^\mu T^\nu = 1 \quad (7.3)$$

The unit vector, $N^\mu(\tau)$, orthogonal to the world-line is found by solving

$$g_{\mu\nu} T^\mu N^\nu = 0 \quad (7.4)$$

together with the normalization condition

$$g_{\mu\nu} N^\mu N^\nu = -1 \quad (7.5)$$

In the special case of a Minkowski background, $g_{\mu\nu} = \eta_{\mu\nu} = \text{diag}(1, -1)$, we find $T^\mu = \gamma(1, V)$ where $V \equiv \partial_t X$, and $N^\mu = \gamma(V, 1)$ where $\gamma = 1/\sqrt{1 - V^2}$.

The coordinate τ is along T^μ and ξ is along N^μ . Therefore, in the neighborhood of some fixed point on the world-line, any space-time point can be written as

$$x^\mu = X_0^\mu + \tau T_0^\mu + \xi N_0^\mu \equiv X^\mu(\tau) + \xi N^\mu(\tau_0) \quad (7.6)$$

where the subscript 0 refers to the fixed point on the world-line. Since the energy density in the fields vanishes far from the kink, only the neighborhood of the world-line is relevant for deriving the effective action. Hence ξ is small and to lowest order we can replace τ_0 in the last term by τ to get

$$x^\mu = X^\mu(\tau) + \xi N^\mu(\tau) \quad (7.7)$$

With the coordinate transformation in Eq. (7.7), the world-line metric can be written in the y^a coordinate system

$$h_{ab} = g_{\mu\nu} \partial_a x^\mu \partial_b x^\nu \quad (7.8)$$

Therefore

$$\begin{aligned} h_{00} &= g_{\mu\nu} (\partial_\tau X^\mu + \xi \partial_\tau N^\mu) (\partial_\tau X^\nu + \xi \partial_\tau N^\nu) \\ &= g_{\mu\nu} \partial_\tau X^\mu \partial_\tau X^\nu + O(\xi) \\ h_{01} &= g_{\mu\nu} (\partial_\tau X^\mu + \xi \partial_\tau N^\mu) N^\nu = O(\xi) \\ h_{11} &= g_{\mu\nu} N^\mu N^\nu = -1 \end{aligned}$$

where we have used the orthogonality of $\partial_\tau X^\mu \propto T^\mu$ and N^μ , and the normalization of N^μ . So the determinant of h_{ab} is

$$h = -g_{\mu\nu} (X^\mu) \partial_\tau X^\mu \partial_\tau X^\nu + O(\xi) \quad (7.9)$$

where we have also expanded the background metric around the kink location.

Next we write,

$$\phi(x^\mu) = \phi_0(y^a) + \psi(y^a) \quad (7.10)$$

where ϕ_0 is the static kink profile function in the kink frame coordinates. For example, in the case of the Z_2 kink, $\phi_0 = \eta \tanh(\sqrt{\lambda/2} \eta \xi)$ (see Eq. (1.9)). The field ψ is the departure of the true field configuration from the static kink profile ϕ_0 . The assumption is that the contribution of ψ to the action is small and hence ψ can be used as a parameter for a perturbative expansion.

Now the field theory action is

$$S = \int d^2x \sqrt{-g} L[\phi, \dot{\phi}; g_{\mu\nu}] \quad (7.11)$$

in terms of the Lagrangian density L and $g = \text{Det}(g_{\mu\nu})$. The metric is taken to be a fixed background and the gravitational effects of the wall are ignored. The full problem of gravitating domain walls is significantly more complicated at a technical level [21].

Now we write this action in the kink frame coordinates to get

$$S = S_0 + O(\xi, \psi) \quad (7.12)$$

with

$$\begin{aligned}
 S_0 &= \int d\tau d\xi \sqrt{|h|} L[\phi_0(\xi), \dot{\phi}_0(\xi); h_{ab}] \\
 &= \int d\tau \sqrt{|h|} \int d\xi L[\phi_0(\xi), 0; h_{ab}] \\
 &= -M \int d\tau \sqrt{|h|}
 \end{aligned} \tag{7.13}$$

where M is the mass of the kink. The last equality follows since the solution is static and hence the Lagrangian density equals the energy density up to a sign. The integration of the Lagrangian density then gives the $-M$ factor. The effective action is therefore the action for a point particle, simply given by the length of the world-line. This result can easily be extended to walls (and strings) propagating in higher dimensions, and the leading term in the effective action is proportional to the world volume. Such geometric effective actions are often referred to as ‘‘Nambu-Goto actions.’’ Even if the self-gravity of the domain wall is taken into account, the dominant contribution to the effective action is still the Nambu-Goto action [21].

The next-to-leading order terms in the effective action, denoted by $O(\xi, \psi)$ in Eq. (7.12), have been discussed for domain walls in [138, 21, 73, 28], building on the earlier analysis for strings [57, 105, 72]. The first-order corrections in both ψ and ξ vanish because the field ϕ_0 is a solution of the equation of motion and hence the action is an extremum at ϕ_0 . The lowest non-trivial corrections come at second order in ξ and ψ . An alternative approach to studying domain wall dynamics has been developed in [9].

Finally we remark that the parameter τ can be chosen arbitrarily. Any other world-line coordinate, $\tau'(\tau)$, leaves the effective action invariant. This fact is called ‘‘reparametrization invariance’’ of the action.

7.2 Walls in 3 + 1 dimensions

The location of a domain wall, $X^\mu(\tau, \zeta, \chi)$, is described by three world-volume coordinates $y^a = (\tau, \zeta, \chi)$. Any point, x^μ , can now be written in terms of the ‘‘wall frame coordinates’’ (see Eq. (7.6) and Fig. 7.2)

$$x^\mu = X^\mu(\tau, \zeta, \chi) + \xi N^\mu(\tau, \zeta, \chi) \tag{7.14}$$

where N^μ is the normal to the wall.

The derivation of the Nambu-Goto action proceeds exactly as in the kink case of the last section and we get

$$S_0 = -\sigma \int d^3\rho \sqrt{|h|} \tag{7.15}$$

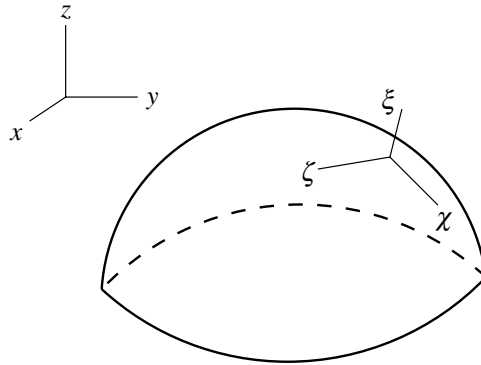


Figure 7.2 A curved section of a domain wall is shown. The world-sheet coordinates are (τ, ζ, χ, ξ) while those in the ambient space (“bulk”) are (t, x, y, z) .

where σ is the energy per unit area (tension) of the wall, the integral is over the wall world volume, $h = \text{Det}(h_{ab})$, and the world-volume metric is

$$h_{ab} = g_{\mu\nu}(X^\rho)\partial_a X^\mu\partial_b X^\nu \quad (7.16)$$

where $a, b = \tau, \zeta, \chi$. Note that the determinant of h_{ab} is positive for the kink in 1 + 1 dimensions and also the domain wall in 3 + 1 dimensions.

The major difference between the kink in 1 + 1 dimensions and the domain wall is that the wall can be curved, and so the profile ϕ_0 , which only applies to planar walls, does not solve the equation of motion. For example, as the wall moves, it accelerates and emits radiation. The radiation part must be treated as a perturbation. However, the analysis is conceptually the same as for the kink and the derivation may be found in [138, 21, 73, 28].

From the Nambu-Goto action for the domain wall, we can derive the equations of motion. The variation of S_0 involves the variation of $h = \text{Det}(h_{\alpha\beta})$. This follows from the identity (see Appendix E)

$$\delta \ln \text{Det} \mathbf{M} = \text{Tr}(\mathbf{M}^{-1} \delta \mathbf{M}) \quad (7.17)$$

valid for any invertible matrix \mathbf{M} . Applying this identity to the matrix h_{ab} we get

$$\delta h = h h^{ab} \delta h_{ab} \quad (7.18)$$

where h^{ab} is the inverse of h_{ab} so that

$$h^{ab} h_{bc} = \delta_c^a \quad (7.19)$$

Therefore the variation of S_0 is

$$\delta S_0 = -\frac{\sigma}{2} \int d^3 \rho \sqrt{|h|} h^{ab} \delta h_{ab} \quad (7.20)$$

We obtain the wall equation of motion by requiring $\delta S_0 = 0$ together with the definition of h_{ab} in Eq. (7.16)

$$\frac{1}{\sqrt{|h|}} \partial_a (\sqrt{|h|} h^{ab} \partial_b X^\sigma) = \Gamma_{\mu\nu}^\sigma h^{ab} \partial_a X^\mu \partial_b X^\nu \quad (7.21)$$

where the Christoffel symbol is defined by the background metric $g_{\mu\nu}$

$$\Gamma_{\mu\nu}^\sigma = \frac{g^{\sigma\rho}}{2} (\partial_\nu g_{\rho\mu} + \partial_\mu g_{\rho\nu} - \partial_\rho g_{\mu\nu}) \quad (7.22)$$

In the special case of a Minkowski background metric, the Christoffel symbol vanishes and

$$\frac{1}{\sqrt{|h|}} \partial_a (\sqrt{|h|} h^{ab} \partial_b X^\sigma) = 0 \quad (7.23)$$

Using Eq. (7.17), the determinant h can be eliminated and the equation of motion can be written as

$$\partial_a (h^{ab} \partial_b X^\sigma) + \frac{1}{2} h^{cd} \partial_a h_{cd} h^{ab} \partial_b X^\sigma = 0 \quad (7.24)$$

The equation of motion for a wall is highly non-linear because h_{ab} itself is defined as a quadratic in derivatives of X^μ . One way to simplify the equations is to choose convenient coordinates. This is possible because the equations of motion of the wall are reparametrization invariant, i.e. we are free to choose any world-volume coordinates (τ, ζ, χ) . A similar situation occurs for strings that have a 1 + 1 dimensional world sheet. There, by a choice of coordinates, the equation of motion can be converted to a simple wave equation in 1 + 1 dimensions together with some quadratic constraints that can be solved quite generally. In the case of the domain wall, however, no such convenient choice of coordinates is known and the equations have not been solved in general. Only a few special solutions are known. Of these, static solutions subject to suitable boundary conditions have minimal surface area, and these have been extensively studied in the mathematics literature e.g. [115].

In a realistic setting, the dynamics of the walls are affected by inter-kink forces, by the interaction of any surrounding particles, the gravitational field of the wall, and the evolution of the background space-time. In addition, there are collisions between different walls, leading to intercommuting (Section 3.8), and annihilation of walls and antiwalls. If there are zero modes on the walls as described in Chapter 5, they could also carry charges and currents and this would introduce other interactions.

7.3 Some solutions

In 1 + 1 dimensions the kink moves like a point particle of mass M . The dynamics are richer in 3 + 1 dimensions where a closed domain wall can oscillate and move in complicated ways. The Nambu-Goto action is valid when the radii of curvature of

the wall and the separation of different sections of wall are both large compared to the thickness of the wall. In addition, the velocity of the wall (in the center of mass frame) should be small. (See Section 7.3.3 for the criterion in the case of collapsing spherical domain walls.) When these conditions are not met, the only way to proceed is to consider the dynamics using the underlying field theory. In this section, we ignore field theory effects and describe some solutions to the Nambu-Goto action.

7.3.1 Planar solutions: traveling waves

A planar domain wall in the $z = 0$ plane is given by

$$X^\mu(\tau, \zeta, \chi) = (\tau, \zeta, \chi, 0) \quad (7.25)$$

Next consider a planar domain wall with some ripples

$$X^\mu(\tau, \zeta, \chi) = (\tau, \zeta, \chi, z(\tau, \zeta, \chi)) \quad (7.26)$$

The function z describes the ripples and we would like solutions for z .

For the wall in Eq. (7.26), the world-volume metric is

$$h_{ab} = \eta_{ab} - \partial_a z \partial_b z \quad (7.27)$$

where

$$\eta_{ab} = \text{diag}(1, -1, -1) \quad (7.28)$$

Inverting h_{ab} is not simple, but inverting η_{ab} is. So consider the “trial” inverse metric

$$\tilde{h}^{bc} = \eta^{bc} + \eta^{bd} \partial_d z \eta^{ce} \partial_e z \quad (7.29)$$

Then by evaluating $h_{ab} \tilde{h}^{bc}$, it can be seen that \tilde{h}^{bc} is the correct inverse metric provided

$$\eta^{ab} \partial_a z \partial_b z = 0 \quad (7.30)$$

Now we can use Eq. (7.24) and the constraint (7.30) to get the equation of motion for the function $z(\tau, \zeta, \chi)$

$$\partial^a \partial_a z = 0 \quad (7.31)$$

Hence any function that satisfies Eqs. (7.31) and (7.30) extremizes the Nambu-Goto action for a domain wall.

Solutions of Eqs. (7.31) and (7.30) have been discussed in [58]. The constraint condition implies that the solution must necessarily be time-dependent. A class of solutions is obtained by noting, for example, that $z = f(\tau - \zeta)$ solves the equation of motion and also the constraint for any choice of function f . This corresponds to a pulse of arbitrary shape on a planar domain wall that propagates in the $+x$

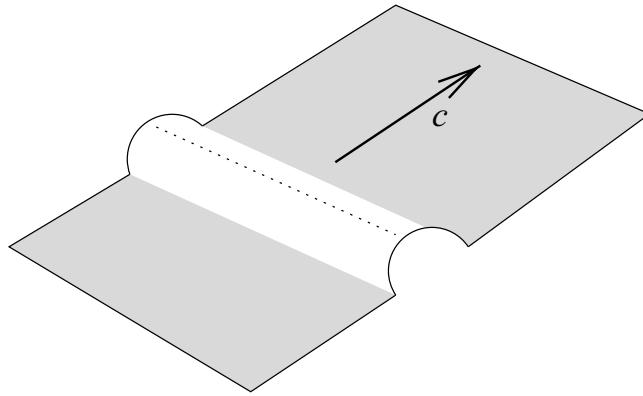


Figure 7.3 Sketch of a traveling wave on a planar domain wall. The pulse propagates at the speed of light along the wall.

direction at the speed of light. Similarly

$$z = f(\tau \pm (n_1\zeta + n_2\chi)), \quad n_1^2 + n_2^2 = 1 \quad (7.32)$$

is a solution for any unit vector (n_1, n_2) . These solutions are known as “traveling waves” (see Fig. 7.3).

Other solutions of the wave equation (Eq. (7.31)) are also known – for example, circular waves – but these do not satisfy the constraint equation and/or have singularities.

7.3.2 Axially symmetric walls

Here we look for a static wall solution in a Minkowski background. The (Cartesian) coordinates of the wall take the form

$$X^\mu(\tau, \theta, \lambda) = (\tau, R(\lambda) \cos \theta, R(\lambda) \sin \theta, \lambda) \quad (7.33)$$

with $\eta_{\mu\nu} = \text{diag}(1, -1, -1, -1)$. The wall metric is seen to be

$$h_{ab} = \text{diag}(1, -R^2, -(1 + R'^2)) \quad (7.34)$$

where R' is the derivative of R with respect to λ . The equation of motion, Eq. (7.21), then leads to

$$\frac{d}{d\lambda} \left(\frac{R}{\sqrt{1 + R'^2}} \right) = 0, \quad \frac{d}{d\lambda} \left(\frac{RR'}{\sqrt{1 + R'^2}} \right) = \sqrt{1 + R'^2} \quad (7.35)$$

with the solution

$$R(\lambda) = \frac{1}{\alpha} \cosh(\alpha\lambda) \quad (7.36)$$

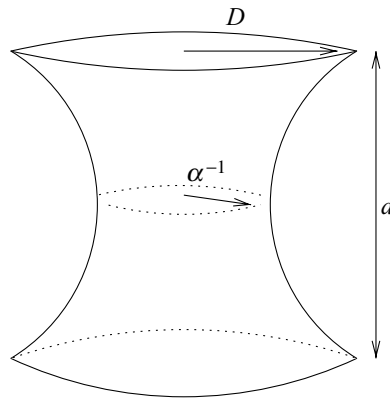


Figure 7.4 Sketch of a catenoid solution.

where α is a parameter, $\tau = t$, $\lambda = z$ and θ is the angle in cylindrical coordinates. Equation (7.36) describes a one-parameter family of static, axially symmetric, domain wall solutions (see Fig. 7.4).

The solution in Eq. (7.36) is a catenoid that is seen in soap films which, like domain walls, also minimize their surface area [23]. Experiments with soap films are done with two parallel circular rings, each of diameter D , placed a certain distance, d , apart. Then the soap film forms a catenoid for $d/D < 0.66$ [117]. Actually there are two catenoid solutions for $d/D < 0.66$ since the relation $\alpha D = \cosh(\alpha d/2)$ has two solutions for α for fixed values of D and d in this regime. A third solution, which consists of two disconnected disks circumscribed by each of the circular rings also exists. For larger values of the separation-to-diameter ratio, d/D , the two-disk solution has less surface area than the catenoid solutions, and the catenoid can pinch off and minimize its area by transforming to the two disks. It seems reasonable to assume that the soap film analysis also applies to the domain wall.

The catenoid is a static solution of the Nambu-Goto equations of motion. It could happen that the catenoid is not a solution of the field equations. A simple example of a solution to the Nambu-Goto equations that does not solve the field equations can be constructed quite easily. Two parallel planar walls (a wall and an antiwall) form a solution to the Nambu-Goto equations but, since these walls have an exponentially small attractive force, they do not form a solution to the field equations. However, by fixing the boundary conditions (as in the soap film case by the rings), the catenoid solution for domain walls has been constructed numerically by solving the equations of motion for the scalar field in the Z_2 model (Sutcliffe, P., 2005, private communication). The stability of the catenoid solution to the Nambu-Goto equations is an open question (Section 7.7).

Quite complicated static domain wall solutions have also been studied in the context of quasicrystals [137] and microemulsions [70].

In addition to static solutions, we could seek time-dependent solutions with axial symmetry. The simplest such case would be a cylindrical domain wall whose radius is a function of time. The radius would contract, pass through zero, and then grow again. A similar solution is obtained for spherical walls which we discuss more explicitly in the next section.

To obtain the cylindrical solution, we note that energy is conserved during collapse. The energy per unit length of a cylindrical wall is

$$\Lambda = \frac{\sigma 2\pi R}{\sqrt{1 - \dot{R}^2}} = \text{constant} \quad (7.37)$$

where σ is the energy per unit area of the wall, R is the radius of the cylinder at time t , and an overdot denotes differentiation with respect to t . The square root factor in the denominator takes care of the Lorentz boost.

The conservation of energy (i.e. constancy of Λ), immediately leads to the solution

$$R(t) = R_0 \cos\left(\frac{t}{R_0}\right) \quad (7.38)$$

where $R_0 = \Lambda/\sigma 2\pi$ is the radius when the wall is at rest.

7.3.3 Spherical walls

Our final example of domain wall solutions is with a spherical ansatz

$$X^\mu(\tau, \theta, \phi) = (\tau, R(\tau)\hat{\mathbf{r}}) \quad (7.39)$$

where

$$\tau = t, \quad \hat{\mathbf{r}} = (\sin\theta \cos\phi, \sin\theta \sin\phi, \cos\theta) \quad (7.40)$$

and θ, ϕ are spherical angular coordinates. The space-time metric is $\eta_{\mu\nu} = \text{diag}(1, -1, -1, -1)$.

We now find

$$h_{ab} = \text{diag}(1 - \dot{R}^2, -R^2, -R^2 \sin^2\theta) \quad (7.41)$$

where overdots denote derivatives with respect to τ . After some algebra, from Eq. (7.21) we obtain the equation of motion

$$\ddot{R} = -\frac{2}{R}(1 - \dot{R}^2) \quad (7.42)$$

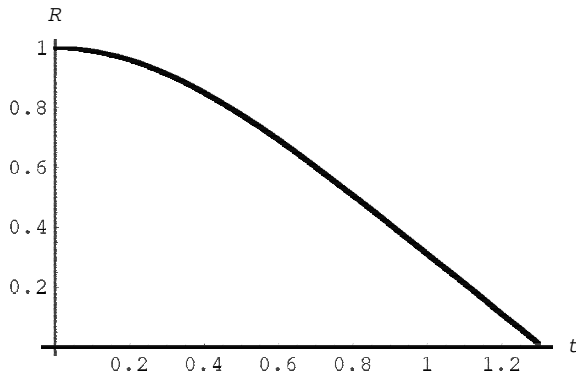


Figure 7.5 Radius of a collapsing spherical domain wall against time in the thin wall approximation. The coordinates in the plot are in units of the maximum radius of the wall.

For $R \neq 0$, $\dot{R}^2 \neq 0, 1$ this can also be written as

$$\frac{d}{d\tau} \left(\frac{R^2}{\sqrt{1 - \dot{R}^2}} \right) = 0 \quad (7.43)$$

which implies

$$4\pi\sigma \frac{R^2}{\sqrt{1 - \dot{R}^2}} = M \quad (7.44)$$

where M is a constant of motion, to be identified with the mass of the spherical domain wall (σ is the mass per unit area of the wall).

The solution can be written in terms of the elliptic integral of the first kind

$$\int_{x_*}^x \frac{dx}{\sqrt{1 - x^4}} = \pm \frac{\tau - \tau_0}{R_0} \quad (7.45)$$

where

$$R_0^2 \equiv \frac{M}{4\pi\sigma}, \quad x \equiv \frac{R}{R_0} \quad (7.46)$$

R_0 has the interpretation of being the radius when the wall is at rest and x_* is the value of x at some initial time τ_0 . The sign in Eq. (7.45) is chosen according to whether one is interested in the expanding or contracting solution. The radius of a collapsing spherical domain wall is plotted in Fig. 7.5.

The behavior of perturbations on the spherical domain wall has been studied in [182]. The result is that at late times the ratio of the perturbation amplitude divided by the radius of the spherical wall, grows as $1/R$ as the wall collapses.

In the Nambu-Goto description, the spherical domain wall oscillates about the center. However, the solution is only valid as long as the thin wall approximation holds. By comparing various terms in the field equations of motion, the thin wall approximation is seen to break down when [183, 73]

$$\frac{R}{R_0} \sim \left(\frac{w}{R_0}\right)^{1/3} \quad (7.47)$$

where w is the wall thickness. This relation is also confirmed by numerically solving the equation of motion in the field theory [183]. In [73], the leading order corrections owing to the thickness and gravity of the spherical domain wall are included, with the conclusion that both these effects tend to slow down the dynamics. The Nambu-Goto action also becomes inadequate owing to radiative losses. As the wall collapses, we expect energy losses owing to radiation and eventually annihilation of the domain wall into radiation. We discuss these processes further in Section 7.5.

The collapse of a zero thickness spherical domain wall is prevented if the background space-time is expanding. Static solutions are obtained if the background is expanding at a constant rate, as in de Sitter space. In a particular coordinate system, the line element for de Sitter space becomes time independent

$$ds^2 = f(r)dt^2 - f^{-1}(r)dr^2 - r^2(d\theta^2 + \sin^2\theta d\phi^2) \quad (7.48)$$

where $f(r) = 1 - H^2r^2$ and H is a constant corresponding to the expansion rate. Following the analysis of [16] for a circular string, the action for a spherical domain wall in the zero thickness limit is

$$S = -4\pi\sigma \int dt R^2 \sqrt{f - \frac{\dot{R}^2}{f}} \quad (7.49)$$

where $R(t)$ is the radius of the spherical wall and $f = f(R)$. Extremization of this action leads to the first integral

$$\dot{R}^2 - f^2 + \epsilon^{-2}R^4 f^3 \equiv \dot{R}^2 + V(R) = 0 \quad (7.50)$$

where $\epsilon = E/4\pi\sigma$ and E is a constant (the first integral). For a static solution we need both $V(R) = 0$ and $V'(R) = 0$ where prime denotes derivative with respect to R . These conditions give the static solution

$$R = H^{-1} \sqrt{\frac{2}{3}} \quad (7.51)$$

with

$$E = \frac{4\pi\sigma}{H^2} \frac{2}{3\sqrt{3}} \quad (7.52)$$

The potential $V(R)$ is a maximum at the location of this solution and therefore the solution is unstable. The instability can be understood without calculation. If the radius of the wall is perturbed to be a little smaller than the value at the solution, the effects of Hubble expansion are weaker while the force owing to curvature is stronger, and so the wall collapses. On the other hand, if the radius is perturbed to be a little larger than the solution value, the expansion effect is stronger while the curvature force is weaker, and the wall expands to yet greater radii.

Planar and spherical domain walls in de Sitter space have been considered in the full field theory in [17, 18]. It is found [17] that instanton solutions describing the nucleation of spherical domain walls exist only when the thickness of the wall is less than $H^{-1}/\sqrt{2}$. This result is also relevant to the problem of finding static thick spherical domain walls in de Sitter space, since an instanton solution can exist only if the static domain wall solution exists (though the converse may not hold). Hence spherical domain wall solutions of the field theory in de Sitter space exist if the domain wall thickness is less than $H^{-1}/\sqrt{2}$.

7.4 Solutions in field theory: traveling waves

The traveling wave solutions discussed in Section 7.3.1 in the zero thickness approximation are also exact solutions to the field equations of motion [160, 161].

Consider the field

$$\phi(t, \mathbf{x}) = \phi_0(z - z_0(t, x, y)) \quad (7.53)$$

where $\phi_0(z)$ is the classical solution for a domain wall in the $z = 0$ plane. We now insert this ansatz in the field theory equation of motion. A little algebra shows that the ansatz is a solution provided

$$\partial_a \partial^a z_0 = 0, \quad (\partial_a z_0)^2 = 0 \quad (7.54)$$

where $a = t, x, y$. These are the same equations obtained above for planar solutions to the Nambu-Goto equations (Eqs. (7.31) and (7.30)). As discussed there, the only non-singular solutions to these equations have the form of traveling waves e.g.

$$z_0(t, x, y) = f(t \pm x, y) \quad (7.55)$$

Hence traveling waves are solutions to the field equations and do not dissipate owing to radiation.²

² It can be shown that traveling waves do not dissipate even when they are considered in quantum field theory [46].

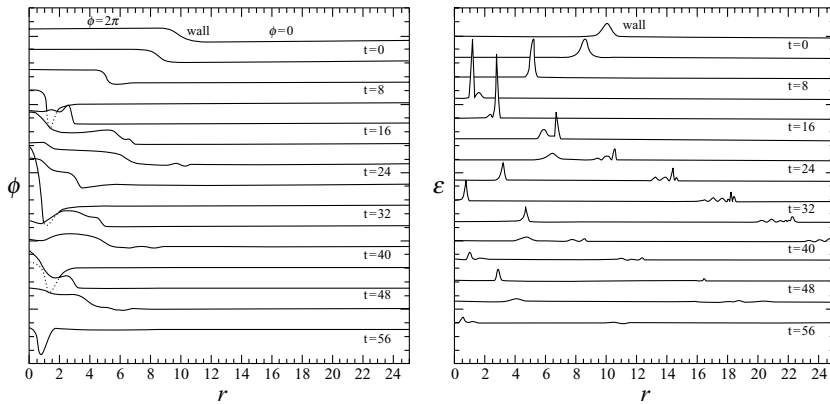


Figure 7.6 Collapse of a spherical sine-Gordon domain wall. The curves in the left-hand plots show the field as a function of radial distance for several different times. The right-hand plot shows the corresponding energy density distributions. [Figure reprinted from [183].]

7.5 Spherical domain walls: field theory

We have seen in Section 3.7 that the collision of a kink and an antikink in $1 + 1$ dimensions leads to chaotic dynamics. The kinks bounce back for certain velocities while for other velocities, both smaller and larger, they annihilate. So we might expect the dynamics of a collapsing spherical domain wall to show similar features. Numerical simulations of the sine-Gordon model show that a collapsing spherical domain wall does not radiate very much energy until it becomes very small (of order the thickness of the wall), then emits a large amount of radiation, then bounces back to form an expanding spherical domain wall (though with less energy than the initial configuration), which then reverses and collapses again (see Fig. 7.6). Simulations of a $\lambda\phi^4$ spherical domain wall, however, do not show any bounce back [183].

7.6 Kink lattice dynamics (Toda lattice)

In Section 6.6.2 we have seen that a phase transition can lead to the formation of a lattice of kinks (Fig. 6.7). What happens if one of the kinks in a lattice collides with a neighboring kink? The interaction potential between neighboring kinks decays exponentially with distance and energy conservation implies that the collision is perfectly elastic. The momentum of the incoming kink is transferred to the target kink [123]. These properties are exactly those assumed for a chain of masses in what is called a “Toda lattice” [155]. The many beautiful properties of a Toda lattice apply to the (one-dimensional) lattice of kinks as well. For example, there are soliton solutions that run along the Toda lattice. So there are also solitons in the dynamical modes of the kink lattice i.e. solitons in the dynamics of solitons!

7.7 Open questions

1. Are there closed domain walls in three dimensions that do not self-intersect as they oscillate? What happens in higher dimensions?
2. Can one show analytically that walls must intercommute on intersection?
3. When traveling waves on domain walls collide, they dissipate some of their energy. Find the energy radiated. Find the energy that goes into excitations of the bound state in the case of the Z_2 wall.
4. Analyze the catenoid domain wall solution and its stability.